Vol 18 No 7, July 2009
1674-1056/2009/18(07)/3079-05

Chinese Physics B

© 2009 Chin. Phys. Soc.
and IOP Publishing Ltd

# Thermal stability of $Mg_2Si$ epitaxial film formed on Si(111) substrate by solid phase reaction*

Wang Xi-Na(王喜娜)[a)b)], Wang Yong(王 勇)[c)], Zou Jin(邹 进)[c)†], Zhang Tian-Chong(张天冲)[a)], Mei Zeng-Xia(梅增霞)[a)], Guo Yang(郭 阳)[a)], Xue Qi-Kun(薛其坤)[a)], Du Xiao-Long(杜小龙)[a)‡], Zhang Xiao-Na(张晓娜)[d)], Han Xiao-Dong(韩晓东)[d)], and Zhang Ze(张 泽)[d)]

[a)] *Beijing National Laboratory for Condensed Matter Physics, Institute of Physics, Chinese Academy of Sciences, Beijing* 100190, *China*
[b)] *Faculty of Physics & Electronic Technology, Hubei University, Wuhan* 430062, *China*
[c)] *School of Engineering and Centre for Microscopy and Microanalysis, The University of Queensland, St Lucia, QLD* 4072, *Australia*
[d)] *Beijing University of Technology, Beijing* 100022, *China*

(Received 5 November 2008; revised manuscript received 5 January 2009)

A single crystalline $Mg_2Si$ film was formed by solid phase reaction (SPR) of a Si(111) substrate with an Mg overlayer capped with an oxide layer(s), which was enhanced by post annealing from room temperature to 100 °C in a molecular beam epitaxy (MBE) system. The thermal stability of the $Mg_2Si$ film was then systematically investigated by post annealing in an oxygen-radical ambient at 300 °C, 450 °C and 650 °C, respectively. The $Mg_2Si$ film stayed stable until the annealing temperature reached 450 °C then it transformed into amorphous $MgO_x$ attributed to the decomposition of $Mg_2Si$ and the oxidization of dissociated Mg.

**Keywords:** $Mg_2Si$, solid phase reaction, thermal stability
**PACC:** 8115

## 1. Introduction

As a narrow-gap semiconductor, the $Mg_2Si$ film has attracted much attention in recent years due to its good ohmic contact character with n-type Si and potential applications in the wavelength ranging between 1.2–1.8 $\mu$m for optical fibres and high-performance thermo-electronic devices.[1−3] Though the growth of polycrystalline $Mg_2Si$ films has been extensively demonstrated by the reactive deposition of Mg onto hot Si substrates or the co-deposition of Mg and Si atoms by molecular beam epitaxy,[4−7] the preparation of a single crystalline $Mg_2Si$ film is still a challenging task. As an important method to synthesize silicide films, solid phase reaction (SPR) of thin metal films with Si substrate has been widely used to study the stability, reaction mechanism, and electronic structure of silicide compounds for Fe, Co and Ni systems,[8−10] in which various silicides with different phases or stoichiometric relations usually form at different stages during annealing temperature variations. It is found that the annealing procedure is an important factor determining the phase formation sequence for multiphase silicides in view of the different bonding energy of metal–Si for the different phases. As for the Mg–Si system, Wigren *et al* and An *et al* reported that the $Mg_2Si$ epitaxial layer could be formed when Mg reacted with Si at the initial stage of the Mg deposition onto the Si(111) substrate at room temperature (RT),[11,12] but the film thickness could not exceed 1 nm and they anticipated that this critical thickness acted as a barrier of mutual diffusion for Mg and Si atoms. They also indicated that it is difficult but possible to prepare $Mg_2Si$ films by the SPR of the pre-deposited Mg film with an underlying Si substrate at relative low temperature. In addition, the Mg silicide has only one stoichiometric phase, i.e. $Mg_2Si$,[6] which makes the control of the SPR of Mg with Si much easier than those of multiphase silicides.

On the other hand, as a main factor influencing

*Project supported by the National Natural Science Foundation (Grant Nos 50532090, 60606023 and 60621091), the Ministry of Science and Technology of China (Grant Nos 2002CB613502 and 2007CB936203) and Australia Research Council.
†E-mail: j.zou@uq.edu.au (Zou Jin)
‡ Corresponding author. E-mail: xldu@aphy.iphy.ac.cn (Du Xiao-Long)

the formation of many silicides formed by SPR,[11,13] the diffusion process highly depends on the annealing temperature and the effect of annealing on the SPR of Mg and Si is still difficult because of the high vapour pressure of Mg even at 200 °C.[7] In addition, the annealing temperature also has a great effect on the stability of Mg–Si bonds in the grown $Mg_2Si$ film,[5] which directly affects its application in optoelectronic and thermoelectric devices. Whereas, up to now, the thermal behaviour of $Mg_2Si$ epitaxial film has been scarcely studied.

In this study, the growth and stability of the $Mg_2Si$ epitaxial film formed by temperature-dependent SPR are systematically investigated with the evolution of microstructure and chemical components confirmed by x-ray photoelectron spectroscopy (XPS), high-resolution transmission electron microscopy (HRTEM), scanning transmission electron microscopy (STEM), energy dispersive spectroscopy (EDS) and electron energy loss spectroscopy (EELS). It is revealed that the $Mg_2Si$ epitaxial film formed by SPR transforms to amorphous $MgO_x$ when the annealing temperature is above 450 °C. The formation mechanism of the $Mg_2Si$ epitaxial film is discussed.

## 2. Experimental

The $Mg_2Si$ films in this study were prepared by controlled SPR of the Mg epitaxial film with Si (111) substrates in an radio-frequency plasma assisted molecular beam epitaxy (MBE) system.[14] Two kinds of samples were prepared according to the flowchart shown by Fig.1. It should be noted that the processes described in the solid frames were carried out in the MBE chamber. For sample A, a low temperature (–10 °C) deposition process of the Mg crystalline film with a thickness of 6 nm was firstly performed in the MBE chamber to suppress the reaction between Mg and Si with a base pressure of $3.0\times10^{-7}$ Pa, followed by depositing a MgO layer with a thickness of 4 nm to protect the Mg film from oxidation, then was annealed at RT in an oxygen-radical (O*) ambient with a pressure of $2\times10^{-3}$ Pa for 20 min. Finally, sample A was taken out from the MBE chamber for XPS depth-profile testment. The test was carried out at RT after $Ar^+$ sputtering for 0 min, 2 min, 3 min and 5 min, respectively. An Al x-ray source was used and the pressure during the XPS testing and sputtering process was held below $10^{-7}$ Pa and $10^{-4}$ Pa, respectively.

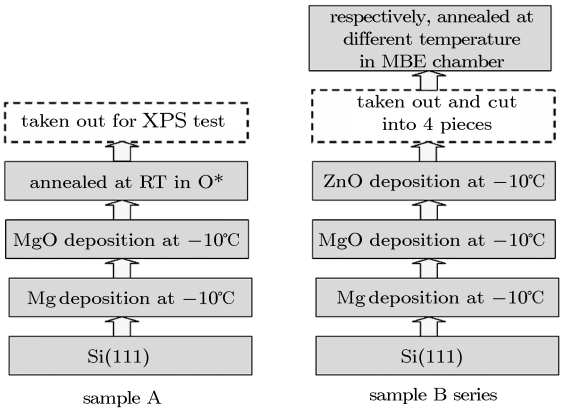



**Fig.1.** A flowchart of the preparation and annealing process for the sample A and sample B series, which includes $B_1$, $B_2$, $B_3$ and $B_4$ with different annealing process, respectively. The processes in solid frames were carried out in the MBE chamber.

Compared with sample A, during the preparation of sample B, an additional ZnO layer with thickness of 100 nm was deposited after deposition of Mg and MgO in order to prevent the re-evapouration of Mg during the subsequent annealing process. The thickness and deposition condition of the Mg and MgO film of sample B are the same as sample A. After the deposition of the ZnO film, sample B was taken out and cut into 4 pieces, then, respectively, re-transferred into the MBE chamber and annealed at different temperatures (namely 100, 300, 450, and 650 °C) for 30 min in an O* ambient with a pressure of $2\times10^{-3}$ Pa. In the following, $B_1$, $B_2$, $B_3$ and $B_4$ will be used to represent four samples annealed at 100, 300, 450 and 650 °C, respectively. The temperature ramping rate during these annealing processes was held within 3 °C/min. Especially, when the temperature reached 100 °C, sample $B_2$, $B_3$ and $B_4$ were kept for 30 min at 100°C, then continuously increased to their corresponding terminal annealing temperature and held for 30 min, respectively. After annealing, the interface structures of samples $B_1$, $B_2$, $B_3$ and $B_4$ were characterized by HRTEM, respectively.

## 3. Results and discussion

From the flowchart of sample A, after deposition of Mg and MgO at –10 °C, a MgO/Mg/Si double-heterostructure (shown by Fig.2(a)) was obtained at –10 °C before sample A was annealed at RT. Since

the preparation of cross-sectional transmission electron microscopy (TEM) specimens for HRTEM observations generally need heating the samples to about 100 °C, it is not possible to examine the structural behaviour without high temperature annealing (such as 100 °C or higher). As a consequence, XPS was carried out at RT for sample A to study the influence of RT annealing on the structural evolution near the Mg/Si interface from –10 °C to RT. Figure 2(b) is the XPS depth-profiles spectra of the Mg 2p core level of sample A at RT, and Fig.2(c) is a sketch illustrating the multilayer structure of sample A at RT. In the case of the non-sputtering, the peak located at 50.4 eV indicates that the film surface is mainly composed of MgO.[15] After sputtered for 2 min, the peak shifts to a lower energy of 49.8 eV, suggesting the existence of metallic Mg. After 3 min of sputtering, the peak shifts to 51.4 eV. Showing good agreement with the $Mg_2Si$ peak reported in Ref.[16], in which the Mg 2p peak of $Mg_2Si$ layer shifts by 0.6 eV to higher energy compared with pure Mg film from $E_B$ = 51.0 eV to 51.6 eV.[16] The Mg signal completely disappears after 5 min sputtering, indicating that the $Mg_2Si$ film has been removed completely by $Ar^+$ and a bare Si substrate is left alone. The above result shows that the MgO/Mg/Si double heterostructure at –10 °C (Fig.2(a)) has evolved into a MgO/Mg/$Mg_2Si$/Si triple heterostructure (Fig.2(c)) after annealing at RT, and the MgO, Mg, and $Mg_2Si$ layers are distributed in sequence from the surface to substrate. This analysis suggests that the formation of $Mg_2Si$ firstly appears near the Mg/Si interface

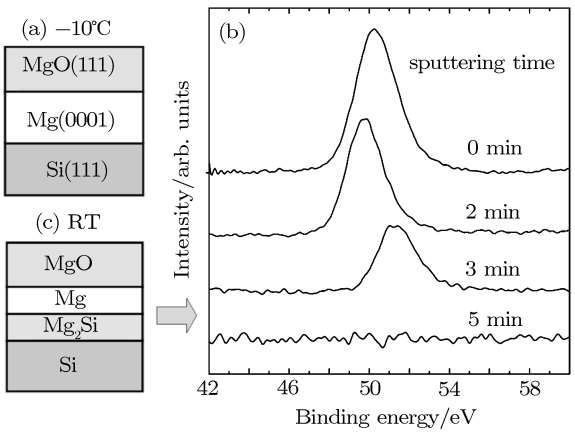



**Fig.2.** (a) A sketch illustrating the multilayer structure of the as-grown sample A at –10 °C; (b) XPS depth-profile spectra of sample A sputtered by $Ar^+$ for different time at RT; (c) A sketch illustrating the multilayer structure of sample A at RT.

region, while the upper part of the original Mg layer has not taken part in the reaction with Si. Since the SPR is realized by the balance between atomic diffusion and the interfacial reaction barrier,[9] the XPS result demonstrates that the diffusivity of Mg or Si atoms at RT is too weak to go through the obtained $Mg_2Si$ film for further reaction. Thus the 6 nm-thick Mg layer and Si can not totally react into $Mg_2Si$. Therefore, it is necessary to increase the diffusivity of Mg or Si atoms by increasing the annealing temperature so as to obtain thicker $Mg_2Si$ epitaxial films, which is confirmed by sample $B_1$.

Figure 3 shows the cross-sectional HRTEM image taken along $[1\bar{1}0]_{si}$ direction near the interface of sample $B_1$. The $Mg_2Si$ (110) film with a uniform thickness of ∼4 nm can be clearly seen sandwiched between the MgO (111) film and the Si (111) substrate, with a spacing of (110) planes (2.2 Å) (1 Å=0.1 nm), which is smaller than that of the MgO (111) planes (2.4 Å). Therefore, the Mg film has completely reacted with the underlying Si atoms at 100 °C, indicating that Mg and Si atoms have enough diffusivity at 100 °C to go across the 4 nm-thick $Mg_2Si$ layer. Figure 3 also shows sharp MgO/$Mg_2Si$ and $Mg_2Si$/Si interfaces and the perfect crystal-quality of the $Mg_2Si$ film.

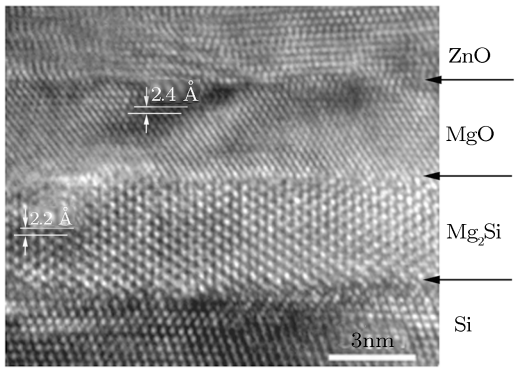



**Fig.3.** Cross-sectional HRTEM micrograph along $\langle 1\bar{1}0\rangle_{Si}$ direction near the interface region of sample $B_1$, of which the ZnO/MgO/Mg/Si triple heterostructure has been annealed at 100 °C.

The annealing temperature was further increased to understand the thermal stability of the $Mg_2Si$ film at high temperatures. Figures 4(a)–4(c) show the cross-sectional HRTEM images along the $[1\bar{1}0]_{si}$ direction near the interface of sample $B_2$, $B_3$ and $B_4$, respectively. As can be seen from Fig.4(a), sharp interfaces of the MgO/$Mg_2Si$/Si double heterostructure remain after annealing at the 300 °C, suggesting that the structure of the $Mg_2Si$ epitaxial film retains stable at 300 °C. Interface degradation is evidenced by

the existence of an amorphous layer between the MgO overlayer and the underlying Si substrate (Figs.4(b) and 4(c)) when the annealing temperature was increased to 450 °C or higher.

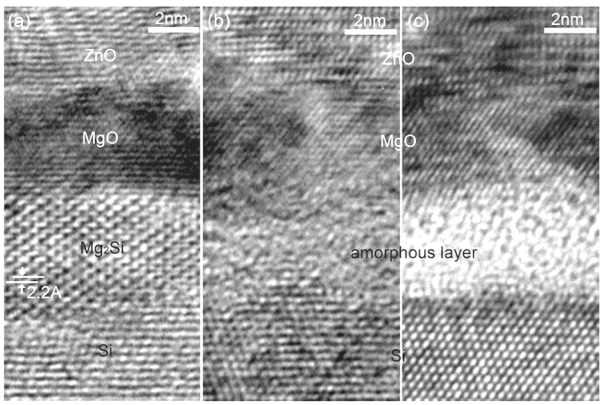



**Fig.4.** Cross-sectional HRTEM micrographs along $\langle 1\bar{1}0\rangle_{Si}$ direction near the interface region of sample $B_2$ (a), $B_3$ (b) and $B_4$(c), of which the ZnO/MgO/Mg/Si triple heterostructure were annealed at 300, 450 and 650 °C, respectively.

To understand the chemical component of the amorphous layer and its formation mechanism, the amorphous layers in samples $B_3$ and $B_4$ were analysed by EDS and EELS. Figure 5(a) is an EDS elemental profile along the interfaces of sample $B_3$, which qualitatively shows the distribution of the elements across the multilayer. Since the thickness of the MgO and Mg films in sample $B_3$ before annealing are about 4 nm and 6 nm, respectively, the amorphous layer and MgO layer should be distributed within the 65–75 nm range along the growth direction in Fig.5(a). From the count variation within the range of 65–70 nm, compared with Mg and O, the signal intensity of Si in the amorphous layer is very poor. The EDS result qualitatively demonstrates that the amorphous layer consists of O and Mg, excluding the obvious existence of Si atoms in the amorphous layer. This was further confirmed by the EELS analysis shown in Figs.5(b) and 5(c). Strong and sharp O-$K$ EELS peaks can be clearly found in the circled area (inset) in Fig.5(b), and Mg-$K$ peak (not shown here) is also observed in the same circled area. From Fig.5(c), the signal of the Si-$L$ peak is neglectable, which proves that there are no obvious Si elements residual in the amorphous layer after annealing at 450 °C. It should be noted that (1) the circled area in Fig.5(b) was selected away from the upper MgO layer to avoid the influence of the O signal from the MgO layer, and (2) the selected area in Fig.5(c) was apart from the Si substrate, so that the interference of the substrate can be kept at a minimum. Taking the EDS and EELS results into account, we can conclude that the amorphous layer is composed of amorphous-$MgO_x$ (A-$MgO_x$). Similar results of EDS and EELS have also been found in sample $B_4$.

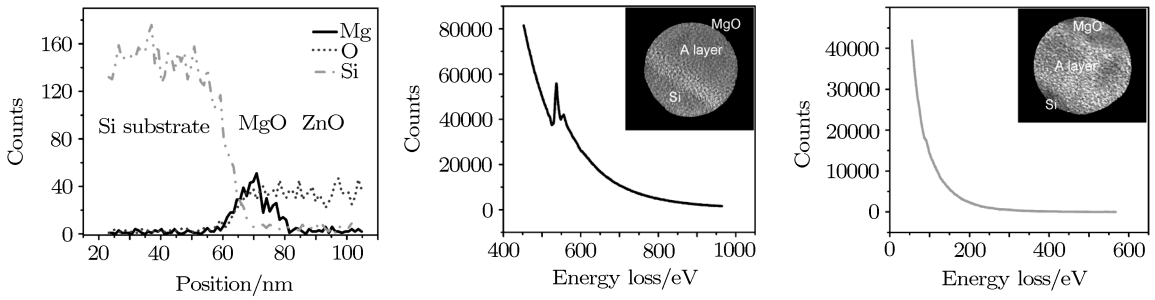



**Fig.5.** Typical elemental profile along the ZnO/MgO/Amorphous layer/Si interface acquired by EDS in the STEM mode (a); EELS profile of O-$K$ (b) and Si-$L$ peak (c) obtained from the circle area (in the inset, where the capital "A" denotes amorphous).

There are two possible reasons for the transformation of $Mg_2Si$ to A-$MgO_x$ at high temperature: (1) oxidation of $Mg_2Si$ and (2) oxidation of Mg after decomposition of $Mg_2Si$. According to the formation heat of $SiO_2$ (–858 kJ·mol$^{-1}$) and MgO (–601 kJ·mol$^{-1}$),[16] it should be much easier for Si than Mg to be oxidized if the oxidation of $Mg_2Si$ occurs. Since the EDS and EELS results exclude the existence of Si, the latter scenario is more reasonable, which indicates that the $Mg_2Si$ film has decomposed at a temperature region of 300–450 °C. This result is consistent with a phenomenon found by Vantomme *et al* – a bare 80 nm-thick $Mg_2Si$ polycrystalline film on Si (111) can be completely removed after annealing at 500 °C in

vacuum.[17] In addition, by using a 200 nm-thick $SiO_2$ film as a cap layer for a 48 nm-thick $Mg_2Si$ polycrystalline film to prevent $Mg_2Si$ desorption, the oxidation of the silicide film was also found after annealing at 500 °C in vacuum attributed to the partial intermixing of silicide with the $SiO_2$ film. From Figs.4(a)–4(c), the thickness and microstructure of both the MgO and ZnO films near the substrate are very stable before and after the $Mg_2Si$ transformation to A-$MgO_x$. So the oxidation of silicide may be related to the O*-rich ambient during annealing and cannot be ascribed to the intermixing with the cap layer in our case. Moreover, it should be noted that the annealing processes of $B_2$, $B_3$ and $B_4$ in the MBE chamber were carried out under O* ambient with a pressure of $2\times10^{-3}$ Pa, which is different from that reported by Vantomme's work.

In order to understand the formation of A-$MgO_x$ after the decomposition of $Mg_2Si$, we note the Mg–Si phase diagram,[6] in which the solid solubility of Si in the Mg solid solution and the solubility of Mg in the Si solid solution are both negligible below 637.6 °C (an eutectic temperature). As a consequence, $Mg_2Si$ decomposition would result in the separation of Mg and Si. The dissociated Si may grow homoepitaxially on the underneath of the Si (111) substrate to reduce the system energy. Simultaneously, strong upward diffusion of Mg may occur due to the high diffusivity of Mg atoms at 450 °C or higher,[5] while the cap layer effectively prevents its evapouration, resulting in the formation of an A-$MgO_x$ layer on the Si substrate. Since the Mg–O bonding in the MgO capping layer and Zn–O bonding in the upper ZnO film are very strong according to their high melting points, the oxygen atoms in the A-$MgO_x$ should come from the O* ambient during the annealing. This also means that the oxidation of the dissociated Mg atoms is most possibly caused by the diffusing-in oxygen atoms through the MgO and ZnO layers from the MBE chamber.

## 4. Summary

The SPR-induced formation and the thermal stability of the $Mg_2Si$ epitaxial film were studied by post annealing of 6-nm-thick Mg epitaxial films capped with a 4 nm-thick MgO layer (in the former case) or a 4 nm-MgO plus 100 nm-ZnO double layer (in the latter case) in O* atmosphere at various temperatures, respectively. The Mg film can totally react with Si and form a 4 nm-thick $Mg_2Si$ epitaxial film due to the enhanced diffusivity of Mg or Si atoms at 100 °C. The decomposition of the $Mg_2Si$ film will occur when the annealing temperature reaches 450 °C, accompanied by oxidization to form A-$MgO_x$. It is possible for the separated Mg atoms after decomposition to stay in the interlayer and react with the oxygen atoms from the atmosphere because of the immiscibility of the dissociated Mg and Si atoms, the oxide cap layer and the O* annealing atmosphere.

## References


[1] Janega P L, McCarffrey J, Landheer D, Buchanan M, Denhoff M and Mitchel D 1988 *Appl. Phys. Lett.* **53** 2056
[2] Akiya M and Nakamura H 1986 *J. Appl. Phys.* **59** 1596
[3] Tani J and Kido H 2005 *Physica* B **364** 218
[4] Takagi N, Sato Y, Matsuyama T, Tatsuoka H, Tanaka M, Fengmin C and Kuwabara H 2005 *Appl. Surf. Sci.* **244** 330
[5] Hosono T, Kuramoto M, Matsuzawa Y, Momose Y, Maeda Y, Matsuyama T, Tatsuoka H, Fukuda Y, Hashimoto S and Kuwabara H 2003 *Appl. Surf. Sci.* **216** 620
[6] Mahan J E, Vantomme A and Langouche G 1996 *Phys. Rev.* B **54** 16965
[7] Vantomme A, Mahan J E, Langouche G, Becker J P, Bael M V, Temst K and Haesendonck C V 1997 *Appl. Phys. Lett.* **70** 1086
[8] Gallego J M and Miranda R 1991 *J. Appl. Phys.* **69** 1377
[9] Vantomme A, Nicolet M A and Theodore N 1994 *J. Appl. Phys.* **75** 3882
[10] Hesse D, Werner P, Mattheis R and Heydenreich J 1993 *Appl. Phys.* A **57** 415
[11] Wigren C, Andersen J N and Nyholm R 1993 *Surf. Sci.* **289** 290
[12] An K S, Park R J, Kim J S and Park C Y 1995 *J. Appl. Phys.* **78** 1151
[13] Calandra C, Bisi O and Ottaviani G 1985 *Surf. Sci. Rep.* **4** 271
[14] Wang X N, Wang Y, Mei Z X, Dong J, Zeng Z Q, Yuan H T, Zhang T C, Du X L, Jia J F, Xue Q K, Zhang X N, Zhang Z, Li Z F and Lu W 2007 *Appl. Phys. Lett.* **90** 151912
[15] Aswal D K, Muthe K P, Tawde S, Chodhury S, Bagkar N, Singh A, Gupta S K and Yakhmi J V 2002 *J. Cryst. Growth* **236** 661
[16] Brause M, Braun B, Ochs D, Maus-Friedrichs W and Kempter V 1998 *Surf. Sci.* **398** 184
[17] Vantomme A, Langouche G, Mahan J E and Becker J P 2000 *Microelectronic Engineering* **50** 237